© 2018 IJSRST | Volume 5 | Issue 3 | Print ISSN: 2395-6011 | Online ISSN: 2395-602X
Themed Section: Science and Technology

Numerical Modeling of Dynamically Excited Non-Resonant Piezoelectric Sensor

R. Abishek[1],V. Shrikanth[2]
Department of Mechanical Engineering, PES University, Bengaluru, Karnataka, India

ABSTRACT

Mass measurement of the viscoelastic or biological specimen using resonant sensor leads to missing mass effect, which affects the precision mass measurement. The non-resonant piezoelectric sensor is used in the mass measurement of these viscoelastic or biological specimen in order to eliminate the missing mass effect. In the present work, finite element analysis method of numerical modeling has been used to characterize the output of the non-resonant piezoelectric sensor. Finite element analysis of mechanical model and electromechanical coupled model is presented. In the mechanical model, the results obtained by FEA of PZT stack are in good agreement with the analytical results obtained by solving equations of motion. In the electromechanical coupled model, FEA of the non-resonant piezoelectric sensor has been carried out. The simulation results obtained for the electromechanical coupled model agrees with the published experimental results.

Keywords: Non-resonant, PZT, Actuator, Sensor

I. INTRODUCTION

Resonant sensors are used in the precise measurement of small mass because of its high measurement sensitivity at the resonance frequency. Some of the piezoelectric based resonant sensors are micro-resonators[1], micro-cantilevers[2], quartz crystal microbalance(QCM)[3], carbon nanotubes[4]. When the resonant sensors are used in the mass measurement of the biologicalspecimens which are intrinsically viscoelastic in nature, affects the precision mass measurement due to damping effects at the resonance frequency.

Sauerbrey[5] first proposed the use of QCM to measure mass.

Voinovaet al.[6] verified theoretical result on Quartz Crystal Microbalance(QCM) measurement on the supported membrane. Due to various damping effects at the resonance frequency, the accurate mass measurement of viscoelastic material is difficult using the resonant sensor.

Shrikanth and Bobji[7] designed a non-resonant piezoelectricbased mass measurement system that operates at a low frequency in order to overcome the missing mass effect. Shrikanth[8] explained the stiffness controlled operation of a sensor. For the sensor to operate in a non-resonant mode, the frequency ratio should fall under the stiffness control region. Karan Kapooret al.[9] proposed an instrument, off-resonant tunnel fork to measure the rheological response of nanoconfined liquid. Because of its off-resonance operation, measurement can perform over a range of shear amplitude and frequency. Pan et al.[10] developed a new method for the piezoelectric charge constant measurement in shear mode (d_{15}) using non-resonant condition. Tung et al.[11] evaluate an electromechanical coupling factor for two piezoelectric materials (PZT-5A and BZT-50BCT) using finite element modeling.

From the detailed review of the literature related to mass measurement of biological specimen, it can be concluded that, as far as the liquid phase mass measurement is concerned, viscous effects of the mass to be measured and viscosity of the surrounding medium poses difficulty in the mass measurement using resonant sensors and leads to missing mass effect, which can be overcome by using a non-resonant piezoelectric sensor. Irrespective of phase/state of mass to be measured, precise mass measurement can be carried out using the non-resonant piezoelectric based mass sensor.

In the present study, we use finite element modeling method in ANSYS, in order to understand the behavior of dynamically excited Non-resonant piezoelectric sensor by characterizing its output and validate the results.

II. NON RESONANT PIEZOELECTRIC SENSOR

A. Geometry and working principle of the non-resonant piezoelectric sensor

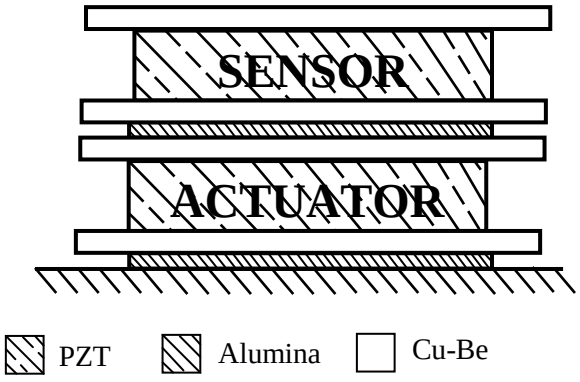

Figure 1. Sectioned view of non resonant piezoelectric sensor

The non-resonant piezoelectric sensor consists of two PZT stacks, one acts as an actuating element and another as a sensing element. Each stack of PZT consists of PZT-5A plate of area 5×5 mm² and thickness 0.75 mm is bonded between two Cu-Be electrode plates of area 5×6 mm and thickness 0.25 mm. A skinny layer of silver based epoxy resin of thickness 50 μm is used to join the interface of PZT and Cu-Be plates. The two stacks of PZT are separated by an alumina layer of area 5×5 mm² and thickness 0.15 mm in order to create electrical isolation. Both the actuator and sensing elements are placed on the mounting block with an alumina layer in between using cyanoacrylate glue.

The actuator element undergoes elastic deformation when a voltage is applied to it, due to indirect piezoelectric effect. $V_{in} = V_0 \cos\omega t$ is the excitation voltage applied to the actuator element, where V_0 is the rms voltage. The distance moved by the sensing element is equal to the elastic deformation of the actuator element. Due elastic deformation of the actuating element and inertia of the sensing element, the charge is generated in the sensing element.

B. Non-resonant mode of operation

Figure 2 shows the frequency response curve of a base excitation system subjected to different damping ratio.

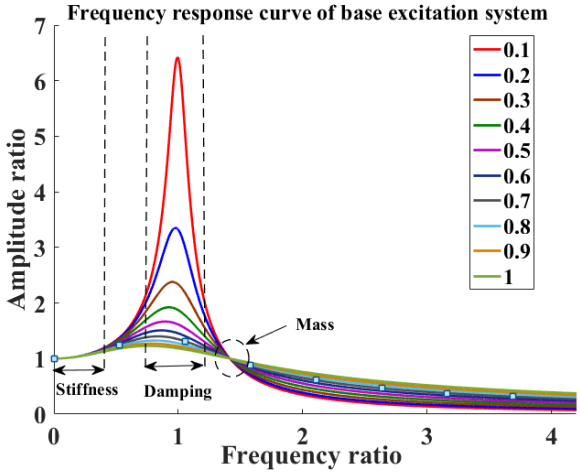

Figure 2. Frequency response curve of base excitation system

The stiffness controlled and the mass controlled region is located before and after the resonance condition respectively, whereas the damping controlled region is located in the resonance condition. In the stiffness and mass controlled region there is no

appreciable increase in the amplitude of vibration due to change in the damping ratio. The frequency ratio in the stiffness controlled region is up to 0.3. As the mass controlled region is a point, the frequency range of operation is limited. The frequency ratio in the mass controlled region is 1.412. For the non-resonant mode of operation, the frequency ratio should fall under stiffness or mass controlled region.

III. PROBLEM FORMULATION

Finite element analysis of non-resonant piezoelectric sensors involves the analysis of mechanical model followed by electro-mechanical coupling model.

The mechanical model involves the finite element analysis of PZT stack. In mechanical model force equivalent to voltage is applied and the results obtained are compared with the analytical results.

Electro-mechanical coupling model involves the finite element analysis of complete non-resonant piezoelectric sensor considering Cu-Be plates, epoxy, alumina and the results obtained are compared with the experimentally published results.

A. Mechanical model

FEA of PZT stack has been carried out under the mechanical model. PZT stack consists of two PZT plates of area 5×5 mm^2 and thickness 0.75 mm. PZT material type used in the analysis is PZT 5A. The bottom plate acts as an actuator and the top plate as a sensor,

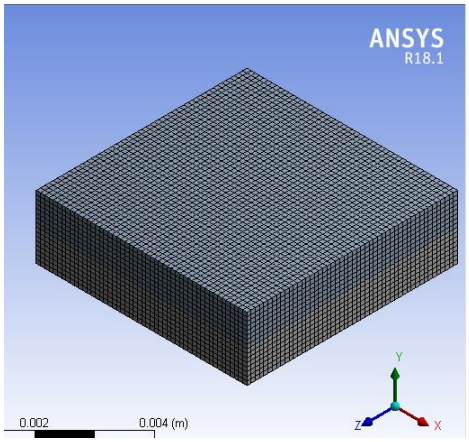

Figure 3. Meshed model of PZT Stack

The meshed model of PZT stack is shown in Figure 3 is a hexahedral mesh consists of 20000 elements with an element size 0.0001m.

Simulation is carried out for the following condition: The bottom face of an actuator is fixed and the force equivalent to voltage is applied to the top face of the actuator element.

B. Electro-Mechanical coupling model

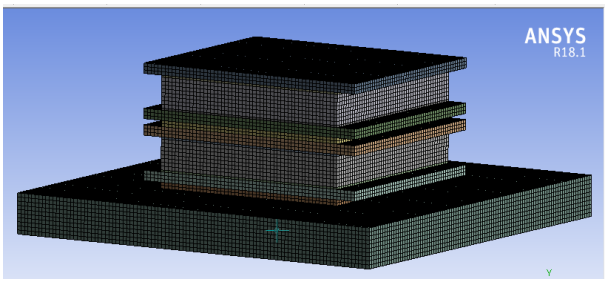

Figure 4. Meshed model of non resonant piezoelectric sensor

FEA of the non-resonant piezoelectric sensor has been carried out under electro- mechanical coupling model. The meshed model of the non-resonant piezoelectric sensor is shown in Figure 4 is a hexahedral mesh consists of 78000 elements with an element size 0.0001m.

Simulation is carried out for the following condition: the mounting block is fixed and the voltage is applied to the top face of the actuator element. For the electrical boundary condition, the bottom surface of

the actuating element should be grounded to create a potential difference.

C. Lumped model of the non-resonant sensor

Figure 5 shows the springs with a mass of the actuator element and sensing element. The force F equivalent to the input voltage is considered.

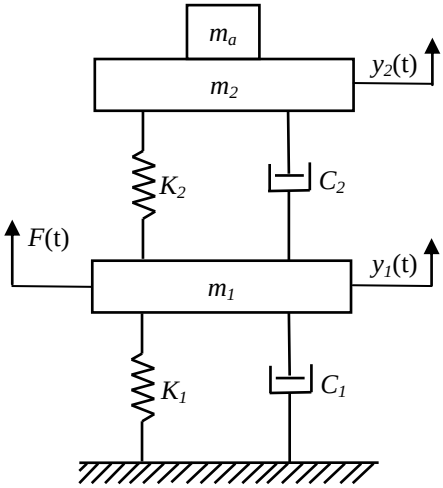

Figure 5. Lumped model of non resonant piezoelectric sensor

For the actuator element, the terms m_1, C_1 K_1 and $y_1(t)$ are the effective mass, effective damping coefficient, effective stiffness and displacement respectively.Similarly for the sensing element, the termsm$_2$, C_2, K_2 and $y_2(t)$ are the effective mass, effective damping coefficient, effective stiffness and displacement of the sensor respectively

The mass m_1 is due to the combined mass of actuator element, sensing element, alumina layer, Cu-Be electrode plates, epoxy resin loaded with silver and super glue.

The mass m_2 is due to the combined mass of sensing element, epoxy, and Cu-Be electrode plate at the top of the Piezo.

With the mass to be measured m_a, m_1, and m_2 can be written as $m_1+m_a= m_1'$ and $m_2+m_a = m_2'$

The differential equations motion of non-resonant piezoelectric sensor are

$$m_1'\ddot{y}_1 + K_1y_1 + C_1\dot{y}_1 - K_2(y_2 - y_1) - C_2(\dot{y}_2 - \dot{y}_1) = F(t), \quad (1)$$

$$m_2'\ddot{y}_2 + K_2(y_2 - y_1) - C_2(\dot{y}_2 - \dot{y}_1) = 0$$

The displacement of the actuating element and sensing element can be determined by solving the above equations of motion. Force equivalent to voltage is given by $F_0 = AGd_{15}V_0 / h$, where, A, h, and G are the lateral area, thickness and rigidity modulus of the piezo respectively. and d_{15} is the piezoelectric charge constant.

IV. RESULTS AND DISCUSSION

A. Simulation results of the mechanical model

1) Displacement of PZT stack:

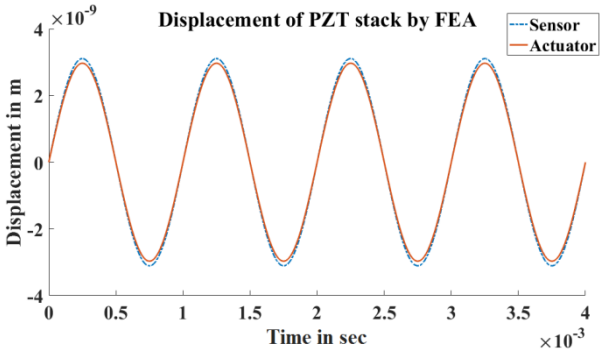

Figure 6(a). Simulation results of PZT Stack

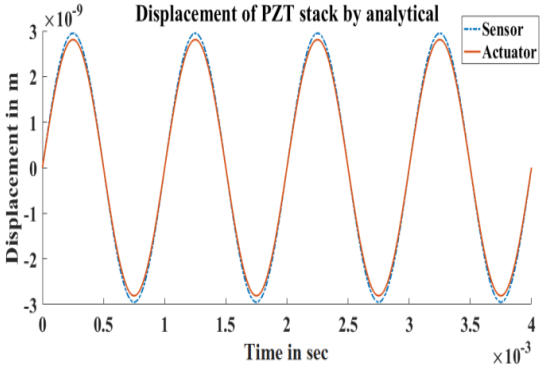

Figure 6 (b). Analytical results of PZT stack

Figure 6 (a) shows the simulation results of PZT stack obtained by FEA in ANSYS. The bottom plate is the actuator element and the top plate is the sensing element. Simulation is carried out for the following condition: sine wave force of magnitude 2.3404 N and frequency 1000 Hz is applied to the top face the actuator element in the Xdirection and the bottom face the actuator element is fixed. The magnitude of force 2.3404 N is equivalent to 5V. Displacements of an actuator and a sensor obtained by simulation are 2.97 nm and 3.11 nm respectively.

Figure 6 (b) shows the analytical results of PZT stack obtained by solving the equation of motion. Displacements of an actuator and a sensor obtained by analytically are 2.95 nm and 2.81 nm respectively. The displacement of a sensor is due to the elastic deformation of the actuating element and inertia of the sensing element. Displacements of PZT stack obtained by simulation and analytical are in good agreement.

2) Undamped frequency sweep of PZT stack

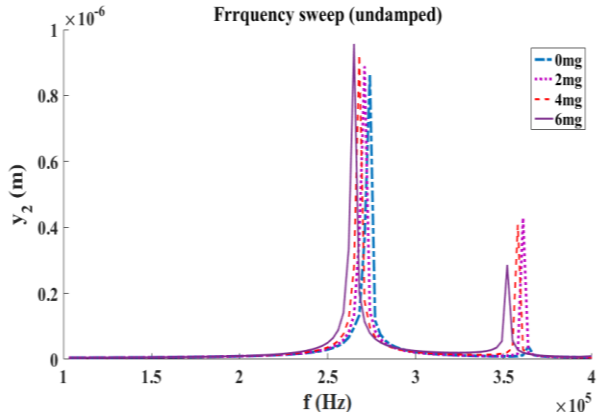

Figure 7. Undamped frequency sweep of PZT Stack for different added mass

Figure 7 shows the frequency sweep of PZT stack for different added mass that is 0mg.2mg,4mg,6mg.

Simulation is carried out for the following condition: the magnitude of the force applied is 2.3404 N on the top face of the actuator element and the bottom face is fixed.

By neglecting the damping effect, the first natural frequency obtained by finite element analysis for 0mg, 2mg, 4mg and 6mg added mass is found to be 271 kHz, 269 kHz, 267 kHz and 264 kHz respectively. Second natural frequencies are found to be 364 kHz, 361kHz. 356 kHz and 352 kHz for added mass 0 mg, 2 mg, 4 mg and 6 mg respectively. Both first and second natural frequencies decreasewith increase in the added mass.

3) Frequency sweep of PZT stack for the different damping ratio

Figure 8(a) shows the frequency sweep of PZT stack subjected to different damping ratio from 0.1 to 0.7 in steps of 0.1.

Figure 8(b) shows the normalized frequency sweep of PZT stack subjected to different damping ratio.

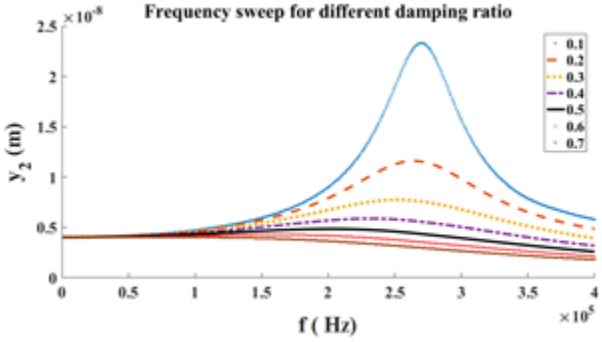

Figure8(a). Frequency sweep of PZT stack subjected todifferent damping ratio.

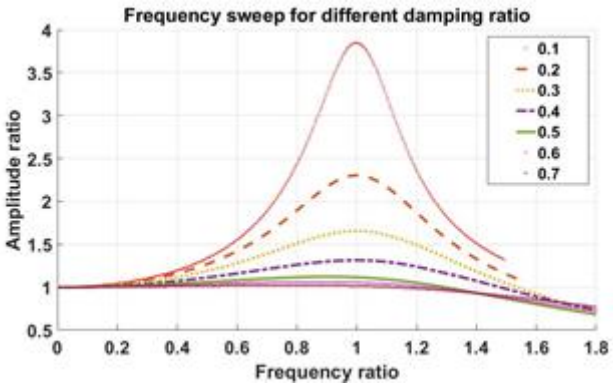

Figure 8(b). Normalised frequency sweep of PZT stack subjected to different damping ratio.

The simulation is carried out by fixing the bottom face of the actuator element and force of 2.3404 N is applied to the top face of the actuator element. It is subjected to different damping ratio from 0.1 to 0.7 in steps of 0.1. The first natural frequency for damping ratio 0.1, 0.2, 0.3, 0.4, 0.5, 0.6 and 0.7 is found to be 270 kHz, 264 kHz, 247 kHz 232 kHz, 202 kHz, 157 kHz and 75 kHz respectively. Beyond 0.7 dampingratio, the negligible amplitude of the sensor is found.

From Figure 8(b) for the frequency ratio less than 0.3, there is no appreciable increase in the amplitude of the sensor due to change in the damping ratio. It is called stiffness control region. As the frequency ratio increases beyond 0.3, the amplitude of the sensor also increases with the change in the damping ratio, which is called damping control region. For the non-resonant mode of operation, the frequency ratio should fall under the stiffness control region.

B. Simulation results of Electro-Mechanical coupled model

1) Mass calibration:

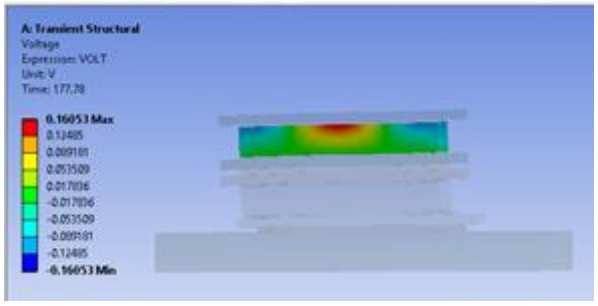

Figure 9(a). Voltage output of sensor without any added mass.

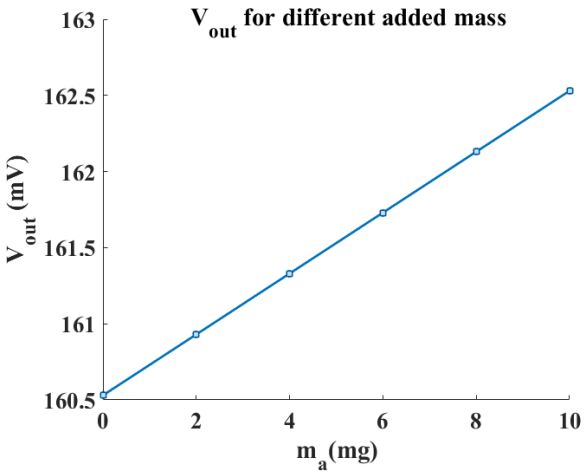

Figure 9(b). Voltage output of sensor for different added mass

Mass calibration is carried out by measuring output voltage for different mass added from 0 mg to 2 mg in steps of 2 mg.

Simulation is carried out for the following operating condition: input voltage of 5V at an excitation frequency 1000 Hz is applied to the actuator element. The output voltage is measured for different added mass from 0 mg to 2 mg in steps of 2 mg.

The voltage output of 0 mg added mass is 160.53 mV. Voltage output increases linearly with increase in the added mass. For every increase in added mass of 2 mg, the voltage output of the sensor is increased by 0.4 mV.

2) Frequency sweep of Non-resonant sensor

Figure 10 shows the frequency sweep of non-resonant piezoelectric sensor obtained by finite element analysis.

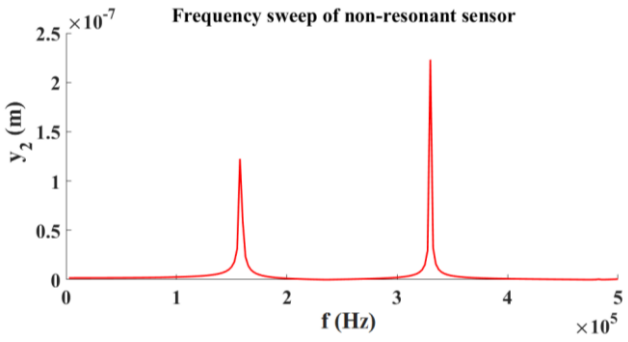

Figure 10. Frequency sweep of non resonant sensor

The frequency sweep of the non-resonant sensor is obtained by simulation for the following condition: input voltage of 5V is applied to the top face of the actuator element and bottom surface is grounded. Neglecting the damping effects, the first and the second natural frequencies obtained are 155 kHz and 340 kHz respectively. The first and the second natural frequencies in the published experimental results are 157 kHz and 350 kHz respectively. Results obtained by FEA agrees with the published experimental result.

V. CONCLUSION

FEA of mechanical and electromechanical coupled model has been carried out.

The displacements of PZT stack obtained by simulation are 2.97 nm and 3.11 nm for the actuator and the sensing element respectively, which are in good agreement with the analytical results obtained for the actuator and the sensing element that is 2.95 nm and 2.81 nm respectively. The first and second natural frequencies obtained for PZT stack by simulation is 271 kHz and 264 kHz respectively.

The voltage output of non-resonant sensor varies linearly with increase in the added mass. For every increase in added mass of 2 mg, the voltage output of sensor increased by 0.4 mV.

The first and the second natural frequencies of the non-resonant sensor considering Cu-Be electrode plates, epoxy and alumina are found be 155 kHz and 340 kHz respectively, which agrees with the published experimental results.

VI. REFERENCES

[1]. A. P. Davila, J. Jang, A. K. Gupta, T. Walter, A. Aronson, and R Bashir, "Microresonator mass sensors for detection of Bacillus anthracis Sterne spores in air and water," Biosensors and Bioelectronics. 22(12), 3028–3035 (2007).

[2]. T. Thundat, E. A. Wachter, S. L. Sharp, and R. J. Warmack, "Detection of mercury vapour using resonating microcantilevers," Applied Physics 66(13), 1695–1697 (1995).

[3]. C. Fredriksson, S. Kihlman, M. Rodahl, and B. Kasemo, "The piezoelectric quartz crystal mass and dissipation sensor: A means of studying cell adhesion," Langmuir 14(2), 248–251 (1998).

[4]. S. Chopra, A. Pham, J. Gaillard, A. Parker, and A. M. Rao, "Carbon nanotube- based resonant-circuit sensor for ammonia," Applied Physics 80(24), 4632–4634 (2002).

[5]. G. Sauebrey, Zeitschrift, Physica Scripta 59,391(1999)

[6]. M.V.Voinova, M. Jonson, B. Kasemo, "Missing mass effect in biodensor's QCM applications", Biosensors and Bioelectronics, 17(10),835-841(2002).

[7]. V. Shrikanth and M. S. Bobji, "A nonresonant mass sensor to eliminate the 'missing mass' effect during mass measurement of biological materials", Review of Scientific Instruments, 84, 105006(2014).

[8]. Shrikanth V, "A nonresonant piezoelectric sensor for mass, force and stiffness measurement", Thesis

[9]. Karan Kapoor, Vinod kanawada, Vibham Shukla, and Shivprasad Patil, "A new tuning fork based instrument for oscillatory shear rheology of nanoconfined liquids", Review of Scientific Instruments, 84(2),0256101(2013).

[10]. W. Y. Pan, W .Y. Gu and L. E. Cross, "Direct Measurement of the Piezoelectric Shear coefficient d15 under non-resonant condition", Materials Letters, 1989.

[11]. Thanh Tung, Nguyen Tinh, Nguyen Hoang, Dang Anh Tuan, "Evaluation of Electrochemical Coupling Factor for Piezoelectric Materials Using Finite Element Modeling", Materials and Chemistry,59-63(2013)